7. A. S. Baranski, W. R. Fawcett, A. C. McDonald, R. M. de Nobriga, and J. R. MacDonald, *ibid.*, **128**, 963 (1981).
8. A. S. Baranski, W. R. Fawcett, and A. C. McDonald, *J. Electroanal. Chem.*, In press.
9. A. S. Baranski, W. R. Fawcett, K. Gatner, A. C. McDonald, J. R. MacDonald, and M. Selen, *This Journal*, **130**, 579 (1983).
10. A. I. Vogel, "Textbook of Quantitative Inorganic Analysis," p. 466, Longmans, London (1961).
11. H. E. Swanson, H. F. McMurdie, M. C. Morris, and E. H. Evans, "Standard X-Ray Diffraction Powder Patterns," Monograph 25, Section 5, p. 13, National Bureau of Standards (U.S.) (1967).
12. J. Black, E. M. Conwell, L. Seigle, and C. W. Spenser, *J. Phys. Chem. Solids*, **2**, 240 (1957).
13. R. N. Bhattacharya and P. Pramanik, *This Journal*, **129**, 332 (1982).

Chemical Etching Characteristics of (001)GaAs

Sadao Adachi and Kunishige Oe

Nippon Telegraph and Telephone Public Corporation, Musashino Electrical Communication Laboratory, Musashino-shi, Tokyo 180, Japan

ABSTRACT

The chemical etching characteristics of (001)GaAs are studied through an SiO_2 (or AZ-1350J photoresist) mask in the solutions of various etching systems: *(i)* HCl, *(ii)* HNO_3, *(iii)* HCl:HNO_3, *(iv)* HBr, *(v)* H_3PO_4, *(vi)* H_2SO_4, *(vii)* HF, *(viii)* Br_2:CH_3OH, *(ix)* NaOCl, and *(x)* alkaline system. The etching profiles are examined by cleaving the wafer in orthogonal directions along the (110) and ($\bar{1}$10) planes. Various etching profiles, such as ordinary-mesa shaped, reverse-mesa shaped structures, and nearly vertical walls, are formed by stripes being etched on the (001) planes. The indexes of the etch-revealed planes are identified by making a comparison with the calculated angle between the (001) surface and etch-side planes. The utility of these etching solutions is also discussed in detail for a variety of GaAs device applications.

Chemical polishing and etching of semiconductors play an essential role in electron device technology and are, therefore, widely employed in the fabrication of many device systems. Chemical etching is used for removing the damage layer of material close to the surface, for producing a high-purity shiny flat surface, and for shaping semiconductor devices, as well as for characterizing structural and compositional features. The electrical and optical properties of semiconductors strongly depend on the dislocation structure in these materials. Certain chemical etchants provide the effect of producing surface features on the semiconductor which can be related to the defects in the crystal. This is essentially true of dislocations, which often form etch pits at their points of intersection with a surface, thus providing a simple way of estimating dislocation densities. A great many techniques have also been described to stain or delineate electrical (pn-junctions) or material interfaces (heterojunctions) of semiconductors by means of chemical etching. Reviews have been published describing some of them (1).

Of the compound semiconductors, GaAs is of great interest because of recent requirements of high-speed transistors, and light sources and detectors for optical fiber communication. From an aspect of device technology, important factors determining the choice of an etchant are in general the etching rate for the material in question (in this case for GaAs), the degree of surface quality and undercutting, the solution chemical aggressiveness toward photoresist masks, and the desired etching profile for the relevant purpose. The most commonly used etchants are various compositions of Br_2:CH_3OH, H_2SO_4:H_2O_2:H_2O, NaOH:H_2O_2:H_2O, and NH_4OH:H_2O_2:H_2O mixtures. Tarui *et al.* (2) have reported preferential etching characteristics of GaAs in the Br_2:CH_3OH system and have discussed a few examples of practical applications of preferential etching for the device-structure design and fabrication (Gunn-effect devices, field-effect devices, and luminescent devices). Selective etching of GaAs in the H_2SO_4:H_2O_2:H_2O system has been studied in detail (3, 4). The etching solutions, NH_4OH:H_2O_2:H_2O (5) and H_3PO_4:H_2O_2:H_2O (6) have also been developed for use in preferential etching of GaAs and the utility of these solutions has been discussed by their application to the fabrication of field effect and bipolar transistors. However, there have been a few reports on device shaping for GaAs by preferential etching. This is a motivation of the present work.

Key words: GaAs, chemical etching, etching profile.

In the present paper, we report the preferential etching characteristics of the (001) surface of GaAs in the solutions of various systems: (*i*) HCl, (*ii*) HNO_3, (*iii*) HCl:HNO_3, (*iv*) HBr, (*v*) H_3PO_4, (*vi*) H_2SO_4, (*vii*) HF, (*viii*) Br_2:CH_3OH, (*ix*) NaOCl, and (*x*) alkaline system. The etching profiles are examined by cleaving the (001)GaAs wafer in orthogonal directions along the (110) and ($\bar{1}$10) planes and are discussed in detail from a crystallographic aspect. The profiles applicable to device-structure design and fabrication are also discussed in detail.

Experimental

Sample.—The GaAs single crystals employed were Si-doped, n-type with carrier densities in the region of 10^{18} cm^{-3}. All wafers used were of (001) surface orientation with an uncertainty of 1° or less. After being mirror-like finished, degreased, and rinsed in deionized water, they were chemically etched in a H_2SO_4:H_2O_2:H_2O = 3:1:1 solution for 30 sec at 80°C. The thickness of these wafers was about 100 μm to permit cleavage for the observation of etching profiles.

Masking pattern.—Etching studies were performed for the etching-selected regions of (001) surface GaAs through windows in an SiO_2 mask (see Fig. 1). The SiO_2 masks used were approximately 2000Å thick and were prepared with conventional sputtering equipment. The desired geometries, in this case the window width of 28 μm wide, were defined by standard photolithography technique using AZ-1350J and an SiO_2 etchant of the HF:NH_4F:H_2O system. Only the HF system, studied in the present work, dissolves the SiO_2 masking pattern. Thus, for this case we used AZ-1350J as a mask of the preferential etching study.

Etching solution.—The etching solutions employed can be classified, for convenience, into the following ten groups: (*i*) HCl system (HCl:CH_3COOH:H_2O_2, HCl:H_3PO_4:H_2O_2, etc.) (*ii*) HNO_3 system (HNO_3:H_2O_2, HNO_3:CH_3COOH, etc.), (*iii*) HCl:HNO_3 system (HCl:HNO_3, (HCl:HNO_3):H_2O, etc.), (*iv*) HBr system (HBr:HNO_3, HBr:HNO_3:H_2O, etc.), (*v*) H_3PO_4 system

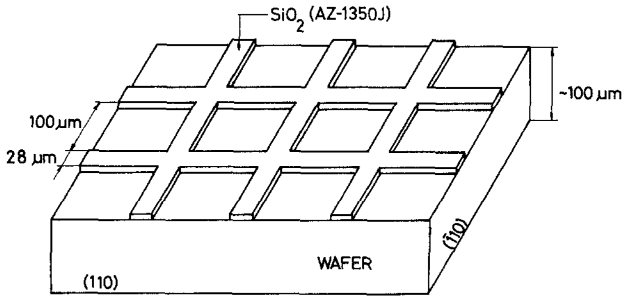

Fig. 1. An SiO_2 (or AZ-1350J) masking pattern on (001)GaAs wafer for chemical etching. The etching profiles are obtained by cleaving the wafer in orthogonal directions along the (110) and (1̄10) planes.

(H_3PO_4:H_2O_2:H_2O, H_3PO_4:CH_3COOH:H_2O_2, etc.), (*vi*) H_2SO_4 system (H_2SO_4:H_2O_2:H_2O, H_2SO_4:CH_3COOH:H_2O, etc.), (*vii*) HF system (HF:HNO_3:H_2O, HF:HNO_3:H_2O_2, etc.), (*viii*) Br_2:CH_3OH system (Br_2:CH_3OH, Br_2:CH_3OH:CH_3COOH, etc.), (*ix*) NaOCl system (NaOCl and NaOCl:HCl), and (*x*) alkaline system (NaOH:H_2O_2:H_2O, NaOH:H_2O_2:H_2O:NH_4OH, etc.). The chemicals used were all of reagent grade. They were as follows: HCl (12*N*), CH_3COOH (17*N*), H_2O_2 (30%), H_3PO_4 (15*N*), $K_2Cr_2O_7$ (purity ≧ 99.8%), HNO_3 (14.5*N*), HBr (9*N*), C_2H_5OH (purity 99.5%), H_2SO_4 (36*N*), HF (50%), Br_2 (purity ≧ 99%), CH_3OH (purity 99.5%), NaOCl aqueous solution (active chlorine min. 5%), NaOH (purity ≧ 96%), NH_4OH (29%), KOH (purity ≧ 86%), and H_2O (deionized water). A large quantity of solution was prepared to prevent the etching temperature from rising and the etch-solution composition from varying during the experiments. Etching was carried out in a temperature-controlled water vessel without illumination. The etchant was freshly mixed prior to each experiment. All etching experiments were done at room temperature without stirring.

Etched depth and etching profile.—After etching, removing the SiO_2 (or AZ-1350J) mask, and rinsing in deionized water, the {110} plane perpendicular to the etched one was cleaved with a razor blade and the etched depths of samples were measured with a calibrated optical microscope. The etched depths were also measured from a step height between the etched and unetched surfaces using an interference microscope. Etching profiles were observed on the (110) and (1̄10) cleavage planes perpendicular to the wafer surface under an optical microscope.

Etching Profile

HCl system.—The etching profiles of (001)GaAs etched in the solutions of the HCl system are shown in Fig. 2: (a) 1HCl:1CH_3COOH:1H_2O_2 (2 min), (b) 1HCl:1H_3PO_4:1H_2O_2 (2 min), (c) 1HCl:1CH_3COOH:1(1*N*-$K_2Cr_2O_7$) (5 min), and (d) 1HCl:1H_3PO_4:1(1*N*-$K_2Cr_2O_7$) (8 min). Note that etchants containing CH_3COOH and H_2O_2 will explode when heated. The cross sections are obtained by cleaving the wafers in orthogonal directions along the (110) and (1̄10) planes (see Fig. 1). The determination of crystallographic directions was made by means of the etch-figure test, where the etch figures were developed on the (001) plane of GaAs by etching in the Br_2:CH_3OH solution through pin-hole windows in an SiO_2 mask (7). The bars drawn in the top of the figure correspond to the masking-pattern length (28 μm).

It is clear from the figure that the etching profiles change in shape with a crystallographic rotation of 90° about the <001> axis and that they exhibit clear crystal habits. The profiles of the (110) cleavage planes [Fig. 2(a), (b), and (c)] exhibit the reverse-mesa shaped planes forming an angle of about 110° with respect to the (001) surface planes. The profiles of the (1̄10) cleavage planes [Fig. 2(a), (b), and (c)] indicate the inclined planes whose sides form an angle of about 55° [Fig. 2(a) and (b)] or 45° [Fig. 2(c)] with respect to the (001) surface planes. The 1HCl:1H_3PO_4:1(1*N*-$K_2Cr_2O_7$) solution did not provide etch depth for an accurate etching-profile observation. One can, however, barely find from Fig. 2(d) that the etchant produces the ordinary-mesa shaped planes for both the (110) and (1̄10) cleavage planes. The 1HCl:1CH_3COOH:1H_2O_2 [Fig. 2(a)] and 1HCl:1H_3PO_4:1H_2O_2 solution [Fig. 2(b)] exhibit that the side-etch speed (undercutting rate) of the (110) cleavage planes is much faster than that of the (1̄10) cleavage planes. It was also found that the HCl:CH_3COOH (or H_3PO_4) solution does not etch GaAs but addition of H_2O_2 to the solution enables the etching of this material. As may be clearly seen in Fig. 2(a) and (b), the solutions produce a microscopic roughness on the etched-bottom surfaces of GaAs. The 1HCl:1CH_3COOH:1(1*N*-$K_2Cr_2O_7$) [Fig. 2(c)] and 1HCl:1H_3PO_4:1(1*N*-$K_2Cr_2O_7$) solution [Fig. 2(d)], on the other hand, provide high quality etched surfaces without any undesirable roughness or etch pits.

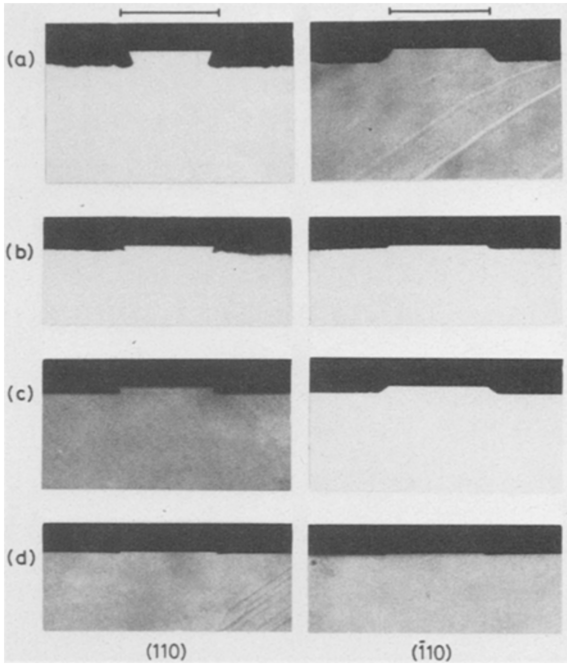

Fig. 2. Etching profiles of (001)GaAs etched in the solutions of the HCl system: (a) 1HCl:1CH_3COOH:1H_2O_2 (2 min), (b) 1HCl:1H_3PO_4:1H_2O_2 (2 min), (c) 1HCl:1CH_3COOH 1(1*N*-$K_2Cr_2O_7$) (5 min), and (d) 1HCl:1H_3PO_4:1(1*N*-$K_2Cr_2O_7$) (8 min). The bars drawn in the top of the figure correspond to the masking pattern length (28 μm).

There have been a few reports on the etching characteristics of GaAs with HCl-based etchants [HCl:Fe^{+++} (8) and HCl:H_2O_2:H_2O (9)]. The HCl:CH_3COOH: (1*N*-$K_2Cr_2O_7$) solution does not erode photoresists such as AZ-1350J and gives high quality surfaces. This new solution can, thus, be used as an etchant of GaAs for producing a shiny flat surface as well as for shaping the samples. Details of this solution will be presented in the near future.

HNO_3 system.—It is known that the Ga{111} plane of GaAs etches unsatisfactorily in most etchants. The Ga{111} plane can, however, be polish-etched like the As{111} surface with the HNO_3:H_3PO_4 solution at 60°C (10). The HNO_3:H_2O solution can also be utilized as a stain etchant to delineate the pn-junction position (11). The etching profiles of (001)GaAs etched in the solutions of the HNO_3 system are shown in Fig. 3: (a)

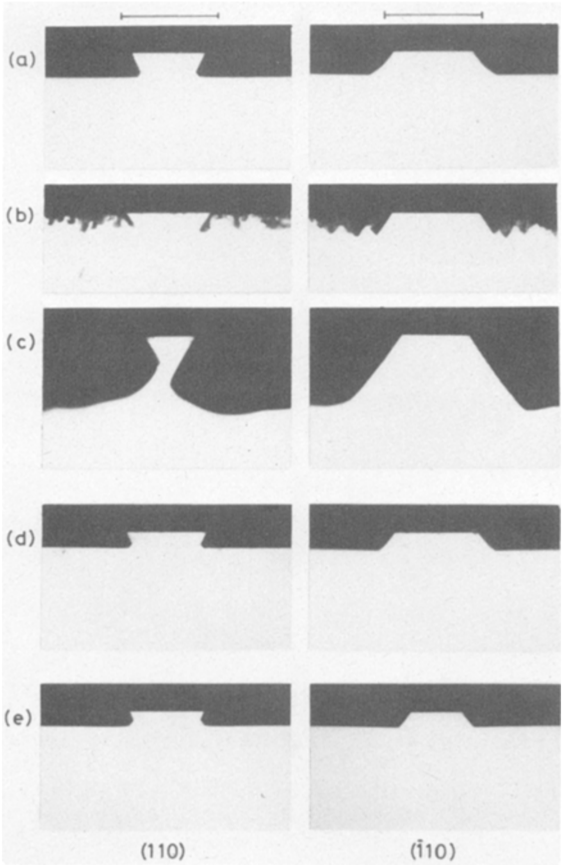

Fig. 3. Etching profiles of (001)GaAs etched in the solutions of the HNO_3 system: (a) $1HNO_3{:}1H_2O_2$ (1 min), (b) $1HNO_3{:}1CH_3COOH$ (2 min), (c) 1 $HNO_3{:}1H_3PO_4$ (2 min), (d) 1 $HNO_3{:}1CH_3COOH{:}1H_2O_2$ (1 min), and (e) $1HNO_3{:}1H_3PO_4{:}1H_2O_2$ (1 min). The bars drawn in the top of the figure correspond to the masking pattern length (28 μm).

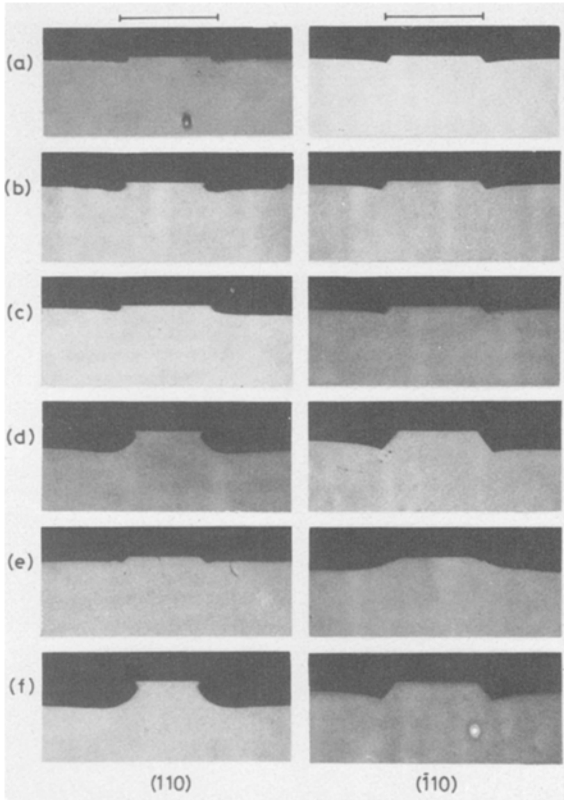

Fig. 4. Etching profiles of (001)GaAs etched in the solutions of the HCl:HNO_3 system: (a) $1HCl{:}1HNO_3$ (2 min), (b) $1HCl{:}2HNO_3$ (2 min), (c) $2HCl{:}1HNO_3$ (4 min), (d) $1(1HCl{:}1HNO_3){:}1H_2O$ (6 min), (e) $1(1HCl{:}1HNO_3){:}1H_2O_2$ (2 min), and (f) $1(1HCl{:}1HNO_3){:}1CH_3COOH$ (4 min). The bars drawn in the top of the figure correspond to the masking pattern length (28 μm).

$1HNO_3{:}1H_2O_2$ (1 min), (b) $1HNO_3{:}1CH_3COOH$ (2 min), (c) $1HNO_3{:}1H_3PO_4$ (2 min), (d) $1HNO_3{:}1CH_3COOH{:}1H_2O_2$ (1 min), and (e) $1HNO_3{:}1H_3PO_4{:}1H_2O_2$ (1 min). In the case of the (110) cleavage planes, the etching profiles of Fig. 3(a), (d), and (e) exhibit two individual etch-revealed planes, *i.e.*, reverse-mesa shaped planes forming an angle of about 115° and ordinary-mesa shaped planes forming an angle of 55° with respect to the (001) surface planes, followed by the flat-bottomed surface planes. The profiles shown in Fig. 3(b) and (c), on the other hand, indicate only the crystal-habit planes forming an angle of about 120° with respect to the (001) surface planes. In the case of the $(\bar{1}10)$ cleavage planes, the profiles [Fig. 3(a)-(e)] indicate the ordinary-mesa shaped planes whose sides form an angle of 55° with respect to the (001) surface planes. The etch-revealed planes of Fig. 3(b), (c), and (e) [$(\bar{1}10$ cleavage planes] indicate clear crystal habits. The $1HNO_3{:}1H_2O_2$ (a), $1HNO_3{:}1CH_3COOH{:}1H_2O_2$ (d), and $1HNO_3{:}1H_3PO_4{:}1H_2O_2$ solution (e) provide high quality etched surfaces with well-defined profiles and flat etched bottoms. The $1HNO_3{:}1CH_3COOH$ (b) and $1HNO_3{:}1H_3PO_4$ solution (c), on the other hand, provide conspicuous roughness on the etched-bottom surfaces.

HCl:HNO_3 system.—The etching profiles of (001)GaAs etched in the solutions of the HCl:HNO_3 system are shown in Fig. 4: (a) $1HCl{:}1HNO_3$ (2 min), (b) $1HCl{:}2HNO_3$ (2 min), (c) $2HCl{:}1HNO_3$ (4 min), (d) $1(1HCl{:}1HNO_3){:}1H_2O$ (6 min), (e) $1(1HCl{:}1HNO_3){:}1H_2O_2$ (2 min), and (f) $1(1HCl{:}1HNO_3){:}1CH_3COOH$ (4 min). The etching profiles of the (110) cleavage planes [Fig. 4(a)-(d) and (f)] exhibit the reverse-mesa shaped structures with roundish tails at the etched bottoms, where the reverse-mesa walls form an angle of about 110° with respect to the (001) surface planes. The profiles of the $(\bar{1}10)$ cleavage planes [Fig. 4(a)-(d) and (f)] indicate the inclined planes forming an angle of 55° with respect to the (001) surface planes, similar to those of the HNO_3 system (see Fig. 3). The etching profiles of Fig. 4(e), on the other hand, do not exhibit clear crystal habit for both the (110) and $(\bar{1}10)$ cleavage planes. It is clear from Fig. 4 that the degree of undercutting for the direction along the $[\bar{1}10]$ axis is larger than for the direction along the [110] axis. The optical microscope images indicate that the HCl:HNO_3 system, except $1(1HCl{:}1HNO_3){:}1H_2O$, produces microscopic roughness on the etched-bottom surfaces. Only the $1(1HCl{:}1HNO_3){:}1H_2O$ solution [Fig. 4(d)] results in an etch-pit free, high quality surface.

HBr system.—The etching profiles of (001)GaAs etched in the solutions of the HBr system are shown in Fig. 5: (a) $1HBr{:}1HNO_3$ (2 min), (b) $1HBr{:}1HNO_3{:}1H_2O$ (3 min), (c) $1HBr{:}1CH_3COOH{:}1(1N\text{-}K_2Cr_2O_7)$ (1 min), and (d) $1HBr{:}1H_3PO_4{:}1(1N\text{-}K_2Cr_2O_7)$ (2 min). The etching profiles of the (110) cleavage planes [Fig. 5(a), (c), and (d)] indicate the etch-revealed planes which are nearly perpendicular to the (001) surface planes with roundish tails at the etched bottoms. The profiles of the $(\bar{1}10)$ cleavage planes [Fig. 5(a), (c), and (d)] indicate the ordinary-mesa shaped, inclined planes forming an angle of about 55° with respect to the (001) surface planes. The HBr system, such as HBr, $1HBr{:}1HCl$, and $1HBr{:}1H_3PO_4$, does not etch the GaAs sample. The $1HBr{:}1HNO_3$ [Fig. 5(a)] and $1HBr{:}1HNO_3{:}1H_2O$ solution [Fig. 5(b)] produce rugged surfaces on the etched bottoms. The solutions, $1HBr{:}1CH_3COOH{:}1(1N\text{-}K_2Cr_2O_7)$ [Fig. 5(c)] and $1HBr{:}1H_3PO_4{:}1(1N\text{-}K_2Cr_2O_7)$ [Fig. 5(d)], on the other

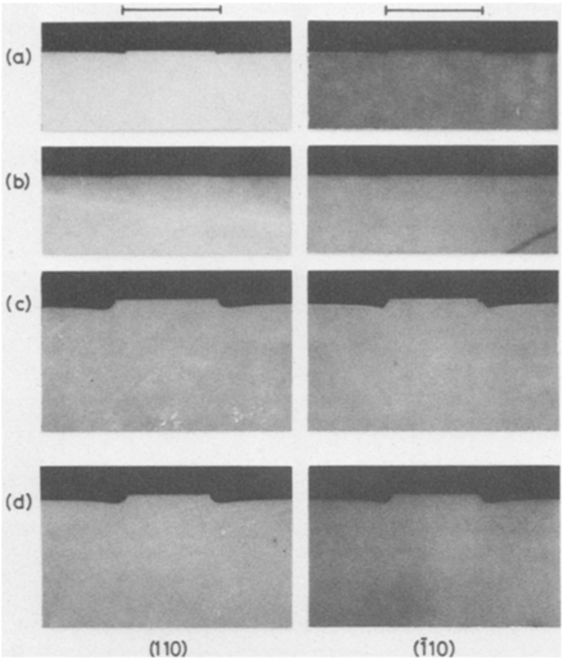

Fig. 5. Etching profiles of (001)GaAs etched in the solutions of the HBr system: (a) 1HBr:1HNO$_3$ (2 min), (b) 1HBr:1HNO$_3$:1H$_2$O (3 min), (c) 1HBr:1CH$_3$COOH:1(1*N*-K$_2$Cr$_2$O$_7$) (1 min), and (d) 1HBr:1H$_3$PO$_4$:1(1*N*-K$_2$Cr$_2$O$_7$) (2 min). The bars drawn in the top of the figure correspond to the masking pattern length (28 μm).

hand, provide relatively smooth etched surfaces without any undesirable etch pits.

Recently, we reported a new chemical solution composed of HBr, CH_3COOH (or H_3PO_4), and a $K_2Cr_2O_7$ aqueous solution for use in etching of InP (12, 13). It was found that this etchant provides high quality etched surfaces without any undesirable roughness or etch pits. The etchant does not erode photoresists such as AZ-1350J, and provides a desirable mesa-shaped structure on the InP and InGaAsP/InP DH (double-heterostructure) wafers with good photoresist-pattern definition. The etching characteristics obtained in the present study are similar to those reported in (12). The HBr:CH_3COOH(or H_3PO_4):$K_2Cr_2O_7$ solution may, thus, be suitable for use in etching of not only the InP but also the GaAs samples.

H_3PO_4 system.—Figure 6 shows the etching profiles of (001) GaAs etched in the solutions of the H_3PO_4 system: (a) $1H_3PO_4$:$1H_2O_2$:$1H_2O$ (2 min), (b) $1H_3PO_4$:$1CH_3COOH$:$1H_2O_2$ (3 min), (c) $1H_3PO_4$:$1CH_3OH$:$1H_2O_2$ (2 min), and (d) $1H_3PO_4$:$1C_2H_5OH$:$1H_2O_2$ (2 min). As can be clearly seen in the figure, the H_3PO_4 system develops the etching profiles which exhibit clear crystal habits. In the case of the (110) cleavage planes, the profiles [Fig. 6(a)-(d)] indicate the reverse-mesa and ordinary-mesa shaped structures, following by the flat-bottomed surfaces. The reverse-mesa and ordinary-mesa planes form angles of about 115° and 55°, respectively, with respect to the (001) surface planes. The etching profiles of the ($\bar{1}$10) cleavage planes [Fig. 6(a)-(d)], on the other hand, exhibit only the inclined sides that slope downward away from the SiO_2 masks. The etch-revealed planes form an angle of about 55° with respect to the (001) surface planes.

A few papers have been published on the etching characteristics of GaAs in the H_3PO_4-based chemical solutions (6, 14). As is shown in this subsection, the H_3PO_4 system provides high quality etched surfaces with well-defined profiles and shiny flat etched bottoms. This system may, thus, be applicable to a wide variety of the device-structure design and fabrication.

H_2SO_4 system.—The H_2SO_4:H_2O_2:H_2O system is known to be one of the most commonly employed etchants for GaAs (3, 4). Chemical polishing by use of this system also gives high quality GaAs surfaces of low index orientations except for the Ga{111} surface. The etching profiles of (001) GaAs etched in the solutions of the H_2SO_4 system are shown in Fig. 7: (a) $1H_2SO_4$:$1H_2O_2$:$1H_2O$ (1 min), (b) $1H_2SO_4$:$1CH_3COOH$:$1H_2O$ (1 min), (c) $1H_2SO_4$:$1H_3PO_4$:$1H_2O$ (1 min), and (d)

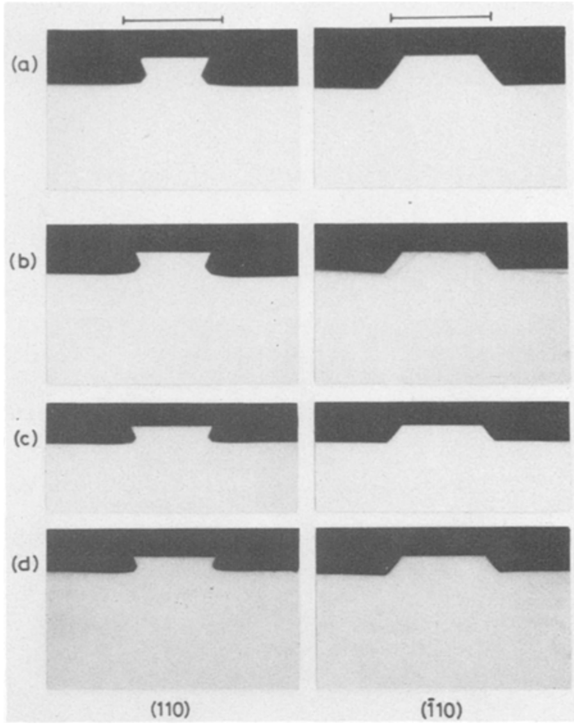

Fig. 6. Etching profiles of (001)GaAs etched in the solutions of the H$_3$PO$_4$ system: (a) 1H$_3$PO$_4$:1H$_2$O$_2$:1H$_2$O (2 min), (b) 1H$_3$PO$_4$:1CH$_3$COOH:1H$_2$O$_2$ (3 min), (c) 1H$_3$PO$_4$:1CH$_3$OH:1H$_2$O$_2$ (2 min), and (d) 1H$_3$PO$_4$:1C$_2$H$_5$OH:1H$_2$O$_2$ (2 min). The bars drawn in the top of the figure correspond to the masking pattern length (28 μm).

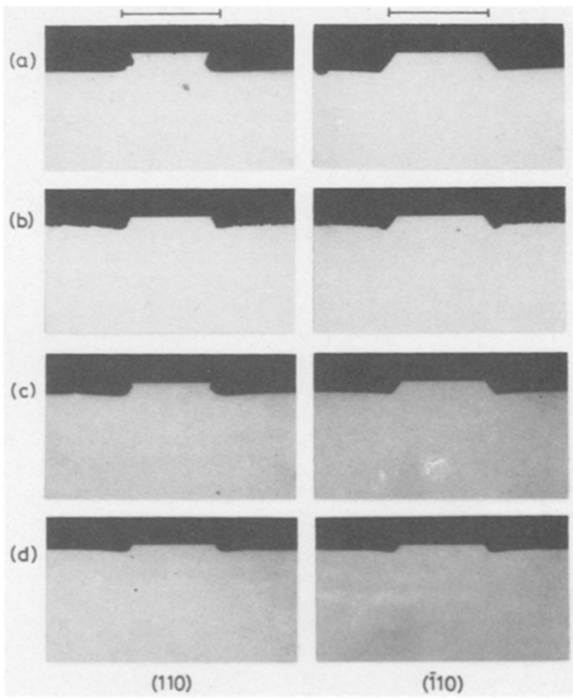

Fig. 7. Etching profiles of (001)GaAs etched in the solutions of the H$_2$SO$_4$ system: (a) 1H$_2$SO$_4$:1H$_2$O$_2$:1H$_2$O (1 min), (b) 1H$_2$SO$_4$:1CH$_3$COOH:1H$_2$O (1 min), (c) 1H$_2$SO$_4$:1H$_3$PO$_4$:1H$_2$O (1 min), and (d) 1H$_2$SO$_4$:1HCl:1(1*N*-K$_2$Cr$_2$O$_7$) (2 min). The bars drawn in the top of the figure correspond to the masking pattern length (28 μm).

$1H_2SO_4$:1HCl:1(1N-$K_2Cr_2O_7$) (2 min). The $1H_2SO_4$:$1H_2O_2$:$1H_2O$ solution for the (110) cleavage plane provides the etch-revealed wall which is composed of two individual reverse-mesa and ordinary-mesa shaped planes. The reverse-mesa and ordinary-mesa planes form angles of about 110° and 55°, respectively, with respect to the (110) surface plane. This solution gives the ordinary-mesa shaped profile for the (110) cleavage plane forming an angle of 55° with respect to the (001) surface plane. The $1H_2SO_4$:$1H_3PO_4$:$1H_2O$ solution for the (110) cleavage plane provides the reverse-mesa plane with roundish tail at the etched bottom. The reverse-mesa shaped plane forms an angle of about 110° with respect to the (001) surface plane. The solution gives the ordinary-mesa shaped profile for the $(\bar{1}10)$ cleavage plane forming an angle of 55° with respect to the (001) surface plane. The $1H_2SO_4$:$1H_2O_2$:$1H_2O$ and $1H_2SO_4$:$1H_3PO_4$:$1H_2O$ solutions provide relatively high quality etched surfaces on the (001)GaAs samples. The $1H_2SO_4$:1HCl:1(1N-$K_2Cr_2O_7$) solution gives the nearly vertical and inclined planes for the (110) and $(\bar{1}10)$ cleavage planes, respectively, with roundish tails at the etched bottoms. This solution also provides relatively high quality etched surface on the (001)GaAs sample. Details of this etching solution can be found in (15).

HF system.—The HF system rigorously attacks the GaAs sample and, as a result, behaves like a fast-speed etchant for this material (16-19). The etching profiles of (001)GaAs etched in the solutions of the HF system are shown in Fig. 8: (a) 1HF:$1HNO_3$:$1H_2O$ (1 min), (b) 1HF:$1HNO_3$:$1H_2O_2$ (15 sec), (c) 1HF:$1HNO_3$:$1CH_3COOH$ (5 sec), (d) 1HF:$1HNO_3$:$1H_3PO_4$ (5 sec), and (e) 1HF:$1H_2SO_4$:$1H_2O_2$ (10 sec). The 1HF:$1HNO_3$:$1H_2O$ [Fig. 8(a)] and 1HF:$1HNO_3$:$1H_3PO_4$ solution [Fig. 8(d)] provide roundish profiles for both the (110) and $(\bar{1}10)$ cleavage planes. The etching profiles of the 1HF:$1HNO_3$:$1CH_3COOH$ solution [Fig. 8(c)] exhibit the roundish and inclined planes for the (110) and $(\bar{1}10)$ cleavage planes, respectively. This inclined plane forms an angle of about 55° with respect to the (001) surface plane. The 1HF:$1HNO_3$:$1H_2O_2$ and 1HF:$1H_2SO_4$:$1H_2O_2$ solutions provide the etching profiles indicating no clear crystal habit [see Fig. 8(b) and (e)].

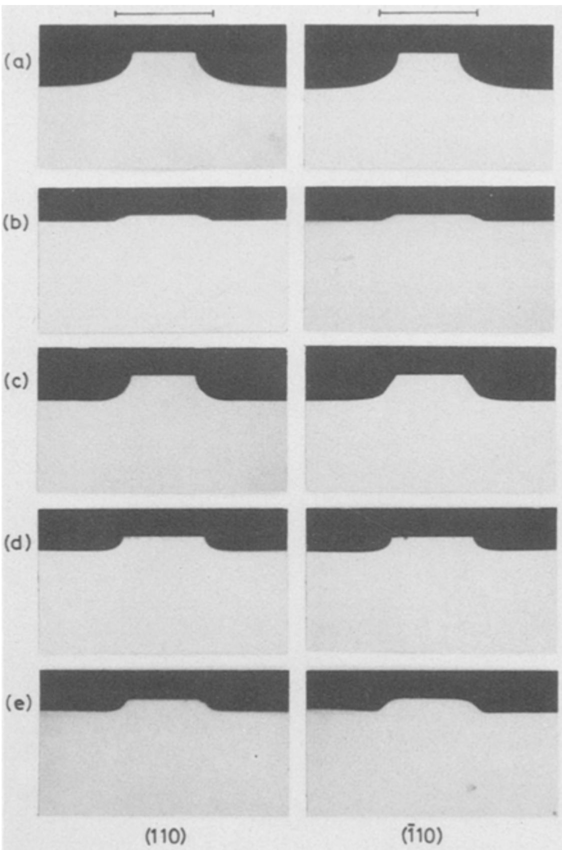

Fig. 8. Etching profiles of (001)GaAs etched in the solutions of the HF system: (a) 1HF:$1HNO_3$:$1H_2O$ (1 min), (b) 1HF:$1HNO_3$:$1H_2O_2$ (15 sec), (c) 1HF:$1HNO_3$:$1CH_3COOH$ (5 sec), (d) 1HF:$1HNO_3$:$1H_3PO_4$ (5 sec), and (e) 1HF:$1H_2SO_4$:$1H_2O_2$ (10 sec). The bars drawn in the top of the figure correspond to the masking pattern length (28 μm).

Br_2:CH_3OH system.—It is known that the Br_2:CH_3OH system gives good results for preferential etching of GaAs (3). The etching rates can be easily controlled by varying the Br_2 concentrations in CH_3OH. Figure 9 shows the etching profiles of (001)GaAs etched in the solutions of the Br_2:CH_3OH system: (a) 4% by volume Br_2:CH_3OH (1 min), (b) 1% by volume Br_2:CH_3OH (3 min), (c) 1(1% by volume Br_2:CH_3OH):$1CH_3COOH$ (5 min), and (d) 1(1% by volume Br_2:CH_3OH):$1H_3PO_4$ (10 min). The Br_2CH_3OH solutions [Fig. 9(a) and (b)] provide that the profiles of the (110) cleavage planes indicate the reverse-mesa shaped structure forming an angle of about 120° with respect to the (001) surface planes while those of the $(\bar{1}10)$ cleavage planes indicate the ordinary-mesa shaped structure forming an angle of 55° with respect to the (001) surface planes. The 1(1% Br_2:CH_3OH):$1CH_3COOH$ solution [Fig. 9(c)] provides the same etching profiles as the Br_2:CH_3OH solutions. Such profiles are the same as those of (001)InP etched with the Br_2:CH_3OH system (7). In the case of the 1(1% Br_2:CH_3OH):$1H_3PO_4$ solution [Fig. 9(d)], the etching profiles exhibit the inclined planes for both the (110) and $(\bar{1}10)$ cleavage planes. The (Br_2:CH_3OH):CH_3COOH and (Br_2:CH_3OH):H_3PO_4 solutions also provide relatively good etched surfaces on GaAs. These solutions may, thus, be used as the slow speed etchants for GaAs.

NaOCl system.—Nonpreferential polishing to obtain high quality GaAs surfaces has been achieved by employing the NaOCl:H_2O solution (20). Figure 10 shows

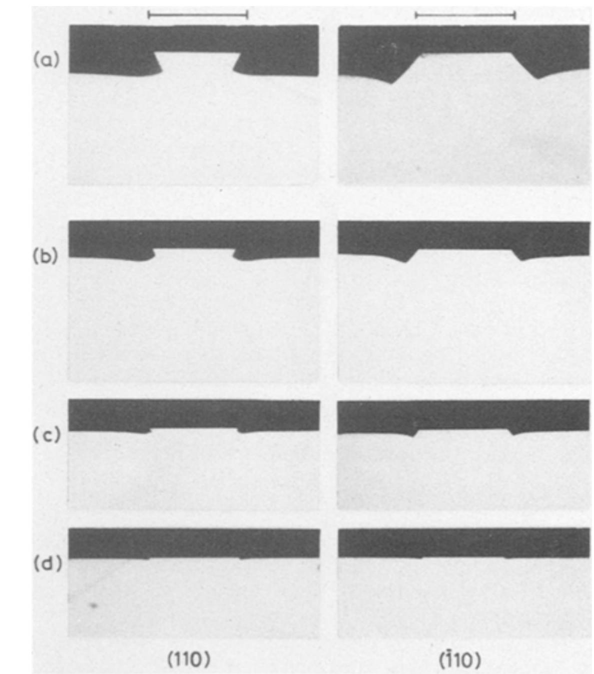

Fig. 9. Etching profiles of (001)GaAs etched in the solutions of the Br_2:CH_3OH system: (a) 4% by volume Br_2:CH_3OH (1 min), (b) 1% by volume Br_2:CH_3OH (3 min), (c) 1(1% by volume Br_2:CH_3OH):$1CH_3COOH$ (5 min), and (d) 1(1% by volume Br_2:CH_3OH):$1H_3PO_4$ (10 min). The bars drawn in the top of the figure correspond to the masking pattern length (28 μm).

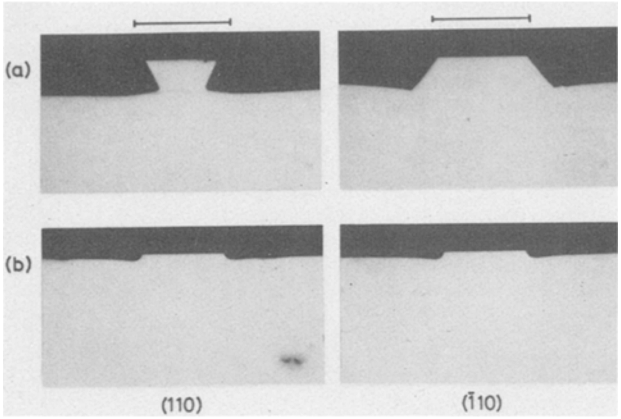

Fig. 10. Etching profiles of (001)GaAs etched in the solutions of the NaOCl system: (a) NaOCl (5 min) and (b) 5NaOCl:1HCl (2 min). The bars in the top of the figure correspond to the masking pattern length (28 μm).

the etching profiles of (001)GaAs etched in the solutions of the NaOCl system: (a) NaOCl (5 min) and (b) 5NaOCl:1HCl (2 min). The etching profile of the (110) cleavage plane [Fig. 10(a)] indicates the reverse-mesa shaped plane forming an angle of about 115° with respect to the (001) surface plane. The profile of the ($\bar{1}$10) cleavage plane [Fig. 10(a)], on the other hand, exhibits the ordinary-mesa shaped plane forming an angle of 55° with respect to the (001) surface plane. Such profiles are the same as those in Fig. 2(a), (c), and Fig. 3(a). The etching profiles of the sample etched with the 5NaOCl:1HCl solution [Fig. 10(b)] indicate the planes which are nearly perpendicular to the (001) surface planes for both the (110) and ($\bar{1}$10) cleavage planes, followed by the roundish tails at the etched bottoms. These profiles are very similar to those in Fig. 8(a) and (d).

Alkaline system.—The alkaline solutions, such as $NaOH:H_2O_2:H_2O$ (21-25) and $NH_4OH:H_2O_2:H_2O$ (5, 26) are the commonly employed etchants for GaAs. The profiles of (001)GaAs etched in the solutions of the alkaline system are shown in Fig. 11: (a) 1(1*N*-NaOH):$1H_2O_2$:$10H_2O$ (4 min), (b) 5(1*N*-NaOH): $1H_2O_2$:$1NH_4OH$ (4 min), (c) $1NH_4OH:1H_2O_2:5H_2O$ (4 min), (d) 1(1*N*-KOH):$1H_2O_2$:$10H_2O$ (4 min), and (e) 5(1*N*-KOH):$1H_2O_2$:$1NH_4OH$ (4 min). The etching profiles of the (110) cleavage planes [Fig. 11(a)-(c) and (e)] indicate the reverse-mesa shaped planes forming an angle of about 110° with respect to the (001) surface planes. The profiles of the ($\bar{1}$10) cleavage planes [Fig. 11(a)-(c) and (e)] indicate the ordinary-mesa shaped, inclined planes whose sides form an angle of about 55° with respect to the (001) surface planes. The alkaline solutions, except $1NH_4OH$: $1H_2O_2$:$5H_2O$, result rough sandpaper textures on the etched bottom surfaces, but the $1NH_4OH:1H_2O_2:5H_2O$ provides a high quality etched surface.

Crystallographic Aspect and Proposed Device Application

In this section, we discuss the etching profiles of (001)GaAs demonstrated in Fig. 2-11 from an aspect of crystallography. The utility of these etching solutions is also discussed for a variety of GaAs device applications.

From a view point of crystallography, we can classify the etching profiles obtained in Fig. 2-11 into the six individual groups, as demonstrated in Fig. 12. The etch-revealed planes forming angles of 110°-115° with respect to the (001) surface planes, observed on the (110) cleavage planes in the solutions of the HCl (Fig. 2) and alkaline system (Fig. 11), correspond to the Ga{$2\bar{2}\bar{1}$} crystallographic planes [see Fig. 12(a)]. The

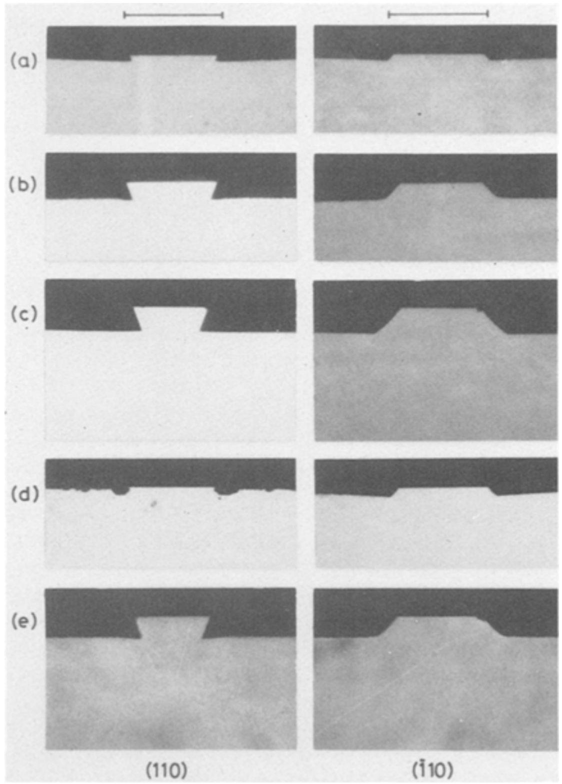

Fig. 11. Etching profiles of (001)GaAs etched in the solutions of the alkaline system: (a) 1(1*N*-NaOH):$1H_2O_2$:$10H_2O$ (4 min), (b) 5(1*N*-NaOH):$1H_2O_2$:$1NH_4OH$ (4 min), (c) $1NH_4OH:1H_2O_2:5H_2O$ (4 min), (d) 1(1*N*-KOH):$1H_2O_2$:$10H_2O$ (4 min), and (e) 5(1*N*-KOH):$1H_2O_2$:$1NH_4OH$ (4 min). The bars drawn in the top of the figure correspond to the masking pattern length (28 μm).

Ga{$2\bar{2}\bar{1}$} crystallographic plane, in principle, forms an angle of 109.5° with respect to the (001) surface plane. The inclined planes forming an angle of about 55° with respect to the (001) surface planes, observed on the (110) cleavage planes in the $1HCl:1CH_3COOH$: $1H_2O_2$ [Fig. 2(a)] and 1(1% $Br_2:CH_3OH$):$1H_3PO_4$ solution [Fig. 9(d)], correspond to the Ga{$1\bar{1}1$} or As{$1\bar{1}1$} crystallographic planes [see Fig. 12(b)]. The {$1\bar{1}1$} crystallographic plane, in principle, forms an angle of 54.7° with respect to the (001) surface plane. The etching profile quite similar to Fig. 12(b) was observed on (001)InP etched in the solutions of the HBr system [HBr and $HBr:H_3PO_4$] (7). The inclined planes forming an angle of about 55° with respect to the (001) surface planes, observed on the ($\bar{1}$10) cleavage planes in the solutions of the various etchant systems [see, *e.g.*, Fig. 11(a)], correspond to the Ga{$\bar{1}\bar{1}1$} crystallographic planes which in principle form an angle of 54.7° with respect to the (001) surface planes. The ordinary-mesa shaped plane forming an inclined angle of about 45°, observed on the ($\bar{1}$10) cleavage plane in the $1HCl:1CH_3COOH$:1(1*N*-$K_2Cr_2O_7$) solution [Fig. 2(c)], may correspond to the {$0\bar{1}1$} crystallographic plane. The plane, in principle, forms an angle of 45° with respect to the (001) surface plane. This plane is a novel one observed on the ($\bar{1}$10) cleavage planes of (001)GaAs. The {$0\bar{1}1$} crystallographic plane was also produced on (001)InP etched in the HBr: H_3PO_4 solution (7).

The etching profile of the (110) cleavage plane, shown in Fig. 12(c), is composed of two individual planes forming angles of 109.5° and 54.7° with respect to the (001) surface plane, while that of the ($\bar{1}$10) cleavage plane exhibits only the mesa-shaped structure forming an angle of 54.7° with respect to the (001) surface plane. These crystallographic planes corre-

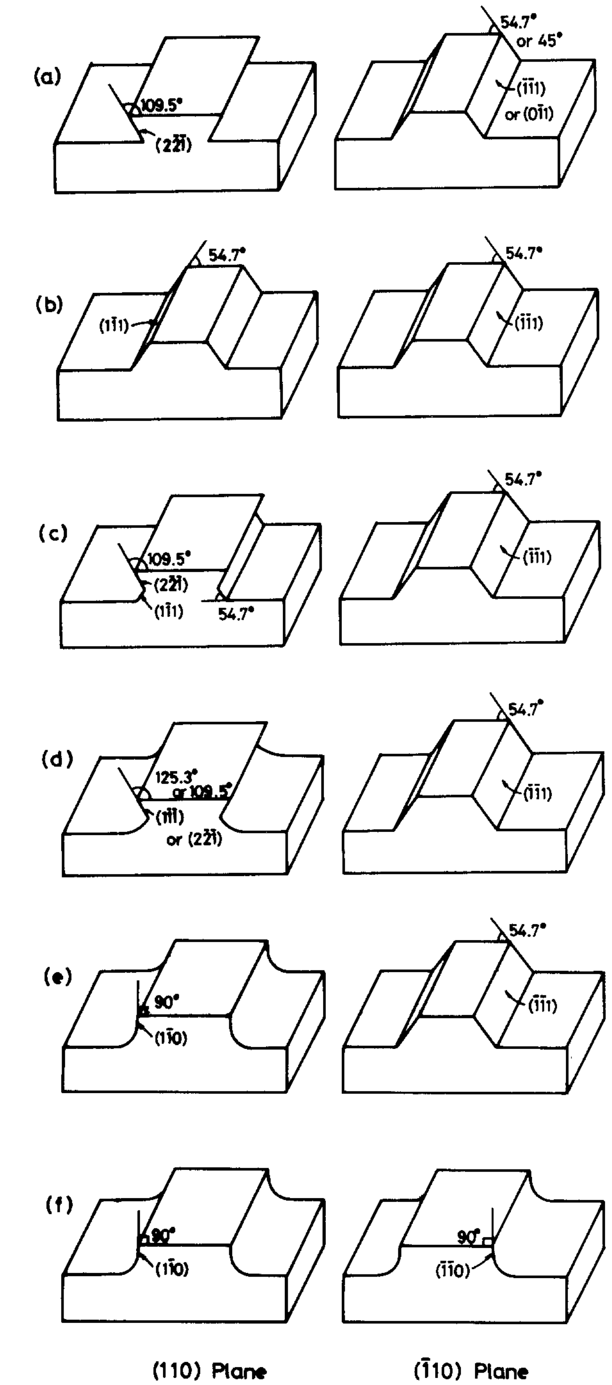

Fig. 12. Schematic diagrams of the etching profiles produced in the (001) planes of GaAs by the various etching solutions (see text).

spond to the Ga{$2\bar{2}\bar{1}$} and Ga{$1\bar{1}1$} or As{$1\bar{1}1$} planes for the (110) cleavage plane and to the Ga{$\bar{1}\bar{1}1$} plane for the ($\bar{1}$10) cleavage plane, respectively. The etchants, HNO_3 [Fig. 3(a), (d), and (e)], H_3PO_4 [Fig. 6(a)-(d)], H_2SO_4 [Fig. 7(a)], and NaOCl system [Fig. 10(a)], provide the etching profiles same as that illustrated in Fig. 12(c). The reverse-mesa and ordinary-mesa shaped structures can be produced on the (110) and ($\bar{1}$10) cleavage planes, respectively, with etchants such as the HNO_3 [Fig. 3(c)] and Br_2: CH_3OH system [Fig. 9(a)-(c)]. These etch-revealed planes form angles of about 120° (reverse-mesa shaped structure) and 55° (ordinary-mesa shaped structure) with respect to the (001) surface planes. The planes can, thus, be identified to be the Ga{111} crystallographic planes. The etching proceeds up to the Ga{111} planes, because the As{111} planes are very active compared with the Ga{111} planes. Consequently, as shown in Fig. 12(d), the Ga{$\bar{1}\bar{1}1$} reverse-mesa and Ga{$\bar{1}\bar{1}1$} ordinary-mesa shaped planes are produced on the (110) and ($\bar{1}$10) cleavage planes, respectively, whose sides in principle form angles of 125.3° (reverse mesa) and 54.7° (ordinary mesa) with respect to the (001) surface planes. The etchants, HCl:HNO_3 [Fig. 4(a)-(d) and (f)] and H_2SO_4 system [Fig. 7(c)], also provide the reverse-mesa and ordinary-mesa shaped profiles for the (110) and ($\bar{1}$10) cleavage planes, respectively. In this case, the reverse-mesa shaped profiles are defined predominantly by the Ga{$2\bar{2}\bar{1}$} slow etching rate faces [see Fig. 12(d)].

The etch-revealed walls perpendicular to the (001) surface planes, obtained on the (110) cleavage planes in the solutions of the HBr [Fig. 5(a), (c), and (d)], H_2SO_4 [Fig. 7(d)], and HF system [Fig. 8(c)], correspond to the {$1\bar{1}0$} crystallographic planes [see Fig. 12(e)]. The etching profiles of the ($\bar{1}$10) cleavage planes revealed by these systems exhibit the ordinary-mesa structures which are defined by the Ga{$\bar{1}\bar{1}1$} crystallographic planes. Some etchants, such as the HF [Fig. 8(a) and (d)] and NaOCl system [Fig. 10(b)], provide the nearly perpendicular walls with respect to the (001) surface planes for both the (110) and ($\bar{1}$10) cleavage planes, followed by the roundish tails at the etched bottoms [see Fig. 12(f)]. This fact clearly suggests that the solutions act isotropically in etching behavior [*i.e.*, they etch the (001)GaAs samples nonpreferentially].

The dissolution process under consideration is far too complex and the available information rather limited to allow a quantitative development of the dissolution mechanism. Moreover, it is difficult to obtain a complete explanation of the difference in the etching profiles with various etching solutions. However, we suggest that this difference is due to the differences of the etching rates in the various crystallographic planes. The etch-revealed planes identified are summarized in Table I along with the etching time and etched depth.

The etching profiles obtained in the present study should be very useful for the design and fabrication of electron devices, such as transistors and Gunn-effect devices. A series of the device-fabrication steps of such devices require various kinds of etchants in accordance with each purpose, *e.g.*, surface cleaning, mesa fabrication, electrical isolation, etc. The etchants mentioned in this paper are, thus, thought to be attractive for a variety of the device-fabrication steps.

Investigations on the subject of ballistic electron transport in submicron semiconductor devices have recently been carried out extensively (27, 28). The ballistic electron transport in semiconductors leads to the realization of low power, high speed switches and high frequency transistors (ballistic Tr's). The realistic ballistic Tr's may have a structure of n^+-n^--n^+ or n^+-p^--n^+ junction diodes, where n^- (or p^-) is the active layer of submicron dimension and n^+ is the source and drain layers. Relevant device technology is, however, very complicated and the gate contact is thought to be difficult to fabricate (27). This problem can be overcome by use of chemical etching. The reverse-mesa shaped profile enables the use of a self-aligned metal evaporation and, therefore, it is possible to fabricate the gate (Schottky) contact on the active layer. The etchants, such as the HCl [Fig. 2(c)], H_3PO_4 [Fig. 6(a)-(d)], H_2SO_4 [Fig. 7(a)], and alkaline system [Fig. 11(c)], are suitable for this use.

A laterally confined structure is required and important in a variety of electro-optic devices, *i.e.*, waveguides, directional couplers, and optical switches, fabricated from GaAs crystals. The etchants, such as the HCl:CH_3COOH:(1*N*-$K_2Cr_2O_7$) [Fig. 2(c)] and HBr: CH_3COOH:(1*N*-$K_2Cr_2O_7$) solution [Fig. 5(c)], are

Table I. The composition of the etchants in parts by volume, etching time, etched depth, and identified crystallographic planes revealed by etching

Etchant	Etching time	Etched depth (μm)	Identified planes (110)	Identified planes ($\bar{1}$10)
1HCl:1CH_3COOH:1H_2O_2	2 min	4.0	$\{2\bar{2}\bar{1}\}$	$\{\bar{1}\bar{1}1\}$
1HCl:1H_3PO_4:1H_2O_2	2 min	1.5	$\{2\bar{2}\bar{1}\}$	$\{\bar{1}\bar{1}1\}$
1HCl:1CH_3COOH:1(1*N*-$K_2Cr_2O_7$)	5 min	2.0	$\{2\bar{2}\bar{1}\}$	$\{0\bar{1}1\}$
1HCl:1H_3PO_4:1(1*N*-$K_2Cr_2O_7$)	8 min	0.3	$\{1\bar{1}1\}$	$\{\bar{1}\bar{1}1\}$
1HNO_3:1H_2O_2	1 min	7	$\{2\bar{2}\bar{1}\}$, $\{1\bar{1}1\}$	$\{\bar{1}\bar{1}1\}$
1HNO_3:1CH_3COOH	2 min		$\{1\bar{1}\bar{1}\}$	$\{\bar{1}\bar{1}1\}$
1HNO_3:1H_3PO_4	2 min	20	$\{1\bar{1}\bar{1}\}$	$\{\bar{1}\bar{1}1\}$
1HNO_3:1CH_3COOH:1H_2O_2	1 min	4.5	$\{2\bar{2}\bar{1}\}$, $\{1\bar{1}1\}$	$\{\bar{1}\bar{1}1\}$
1HNO_3:1H_3PO_4:1H_2O_2	1 min	3.5	$\{2\bar{2}\bar{1}\}$, $\{1\bar{1}1\}$	$\{\bar{1}\bar{1}1\}$
1HCl:1HNO_3	2 min	1.0	$\{2\bar{2}\bar{1}\}$	$\{\bar{1}\bar{1}1\}$
1HCl:2HNO_3	2 min	1.5	$\{2\bar{2}\bar{1}\}$	$\{\bar{1}\bar{1}1\}$
2HCl:1HNO_3	4 min	1.0	$\{2\bar{2}\bar{1}\}$	$\{\bar{1}\bar{1}1\}$
1(1HCl:1HNO_3):1H_2O	6 min	5.0	$\{2\bar{2}\bar{1}\}$	$\{\bar{1}\bar{1}1\}$
1(1HCl:1HNO_3):1H_2O_2	2 min	2.0	*	*
1(1HCl:1HNO_3):1CH_3COOH	4 min	5.0	$\{2\bar{2}\bar{1}\}$	$\{\bar{1}\bar{1}1\}$
1HBr:1HNO_3	2 min	0.5	$\{1\bar{1}0\}$	$\{\bar{1}\bar{1}1\}$
1HBr:1HNO_3:1H_2O	3 min	0.15		
1HBr:1CH_3COOH:1(1*N*-$K_2Cr_2O_7$)	1 min	1.5	$\{1\bar{1}0\}$	$\{\bar{1}\bar{1}1\}$
1HBr:1H_3PO_4:1(1*N*-$K_2Cr_2O_7$)	2 min	2.0	$\{1\bar{1}0\}$	$\{\bar{1}\bar{1}1\}$
1H_3PO_4:1H_2O_2:1H_2O	2 min	8	$\{2\bar{2}\bar{1}\}$, $\{1\bar{1}1\}$	$\{\bar{1}\bar{1}1\}$
1H_3PO_4:1CH_3COOH:1H_2O_2	3 min	6	$\{2\bar{2}\bar{1}\}$, $\{1\bar{1}1\}$	$\{\bar{1}\bar{1}1\}$
1H_3PO_4:1CH_3OH:1H_2O_2	2 min	5.0	$\{2\bar{2}\bar{1}\}$, $\{1\bar{1}1\}$	$\{\bar{1}\bar{1}1\}$
1H_3PO_4:1C_2H_5OH:1H_2O_2	2 min	4.0	$\{2\bar{2}\bar{1}\}$, $\{1\bar{1}1\}$	$\{\bar{1}\bar{1}1\}$
1H_2SO_4:1H_2O_2:1H_2O	1 min	5.0	$\{2\bar{2}\bar{1}\}$, $\{1\bar{1}1\}$	$\{\bar{1}\bar{1}1\}$
1H_2SO_4:1CH_3COOH:1H_2O	1 min	2.5	*	$\{\bar{1}\bar{1}1\}$
1H_2SO_4:1H_3PO_4:1H_2O	1 min	3.0	$\{2\bar{2}\bar{1}\}$	$\{\bar{1}\bar{1}1\}$
1H_2SO_4:1HCl:1(1*N*-$K_2Cr_2O_7$)	2 min	1.5	$\{1\bar{1}0\}$	$\{\bar{1}\bar{1}1\}$
1HF:1HNO_3:1H_2O	1 min	10	$\{1\bar{1}0\}$	$\{\bar{1}\bar{1}0\}$
1HF:1HNO_3:1H_2O_2	15 sec	2.0	*	*
1HF:1HNO_3:1CH_3COOH	5 sec	7	$\{1\bar{1}0\}$	$\{\bar{1}\bar{1}1\}$
1HF:1HNO_3:1H_3PO_4	5 sec	4.0	$\{1\bar{1}0\}$	$\{\bar{1}\bar{1}0\}$
1HF:1H_2SO_4:1H_2O_2	10 sec	3.5	*	*
4% Br_2:CH_3OH	1 min	6	$\{1\bar{1}\bar{1}\}$	$\{\bar{1}\bar{1}1\}$
1% Br_2:CH_3OH	3 min	2.0	$\{1\bar{1}\bar{1}\}$	$\{\bar{1}\bar{1}1\}$
1(1% Br_2:CH_3OH):1CH_3COOH	5 min	1.0	$\{1\bar{1}\bar{1}\}$	$\{\bar{1}\bar{1}1\}$
1(1% Br_2:CH_3OH):1H_3PO_4	10 min	0.2	$\{1\bar{1}1\}$	$\{\bar{1}\bar{1}1\}$
NaOCl	5 min	9	$\{2\bar{2}\bar{1}\}$, $\{1\bar{1}1\}$	$\{\bar{1}\bar{1}1\}$
5NaOCl:1HCl	2 min	1.5	$\{1\bar{1}0\}$	$\{\bar{1}\bar{1}0\}$
1(1*N*-NaOH):1H_2O_2:10H_2O	4 min	1.5	$\{2\bar{2}\bar{1}\}$	$\{\bar{1}\bar{1}1\}$
5(1*N*-NaOH):1H_2O_2:1NH_4OH	4 min	4.5	$\{2\bar{2}\bar{1}\}$	$\{\bar{1}\bar{1}1\}$
1NH_4OH:1H_2O_2:5H_2O	4 min	7	$\{2\bar{2}\bar{1}\}$	$\{\bar{1}\bar{1}1\}$
1(1*N*-KOH):1H_2O_2:10H_2O	4 min	2.0	*	$\{\bar{1}\bar{1}1\}$
5(1*N*-KOH):1H_2O_2:1NH_4OH	4 min	5.5	$\{2\bar{2}\bar{1}\}$	$\{\bar{1}\bar{1}1\}$

* Etching profile does not exhibit clear crystal habits.

thought to be useful for the fabrication of laterally confined electro-optic devices because these solutions provide high quality etched surfaces with good resist-pattern definition. A laterally confined structure is also required especially in a variety of GaAs semiconductor lasers. The lateral confinement structure not only improves laser operation characteristics such as threshold current, stable fundamental transverse mode, and high temperature operation, but also linear light-current characteristics, narrow beam divergence, and high power output. The results presented in this paper show that one can easily obtain various types of laterally confined channels by properly choosing the etching mixtures, its component proportion, channel width, and etching time.

Realization of a monolithic integrated optical circuit is a current topic in the field of injection laser technology. To fabricate the high quality etched mirrors, it is desirable to employ etching solution which provides vertical mirror walls on the etching profile (13). The etching solutions, HBr [Fig. 5(c) and (d)], H_2SO_4 [Fig. 7(d)], HF [Fig. 8(a), (c), and (d)], and NaOCl system [Fig. 10(b)], provide the nearly vertical mirror walls for the (110) cleavage planes and are, thus, thought to be suitable for use in the etched mirror definitions. The etchants may also be widely used in GaAs devices to obtain desirable mesa-shaped structure or to isolate individual device component on one wafer.

Conclusion

We have studied chemical etching characteristics of (001)GaAs in the solutions of various systems: (*i*) HCl, (*ii*) HNO_3, (*iii*) HCl:HNO_3, (*iv*) HBr, (*v*) H_3PO_4, (*vi*) H_2SO_4, (*vii*) HF, (*viii*) Br_2:CH_3OH, (*ix*) NaOCl, and (*x*) alkaline system. The etching profiles exhibiting crystal habits, *e.g.*, ordinary-mesa shaped, reverse-mesa shaped structures, and nearly vertical walls, have been found to be formed by stripes parallel to the $\langle 110 \rangle$ and $\langle \bar{1}10 \rangle$ directions being etched on the (001) planes. The indexes of the etch-revealed planes have been identified by making a comparison with the calculated angle between the (001) surface and etch-side planes. The etching profiles applicable to the device-structure design and fabrication have also been discussed in detail.

Acknowledgment

The authors wish to thank K. Kumabe, S. Hashimoto, and N. Kuroyanagi for their continual encouragement.

Manuscript submitted Feb. 18, 1983; revised manuscript received July 8, 1983.

Nippon Telegraph and Telephone Public Corporation assisted in meeting the publication costs of this article.

REFERENCES

1. B. Tuck, *J. Mater. Sci.*, **10**, 321 (1975); W. Kern, *RCA Rev.*, **39**, 278 (1978).
2. Y. Tarui, Y. Komiya, and Y. Harada, *This Journal*, **118**, 118 (1971).
3. S. Iida and K. Ito, *ibid.*, **118**, 768 (1971).
4. D. W. Shaw, *ibid.*, **128**, 874 (1981).
5. J. J. Gannon and C. J. Nuese, *ibid.*, **121**, 1215 (1974).
6. Y. Mori and N. Watanabe, *ibid.*, **125**, 1510 (1978).
7. S. Adachi and H. Kawaguchi, *ibid.*, **128**, 1342 (1981).
8. H. C. Gatos and M. C. Lavine, *ibid.*, **107**, 427 (1960).
9. E. Biedermann and K. Brack, *ibid.*, **113**, 1088 (1966).
10. J. G. Grabmaier and C. B. Watson, *Phys. Status Solidi*, **32**, K13 (1969).
11. T. H. Yeh and A. E. Blakeslee, *This Journal*, **110**, 1018 (1963).
12. S. Adachi, *ibid.*, **129**, 610 (1982).
13. S. Adachi, Y. Noguchi, and H. Kawaguchi, *ibid.*, **129**, 1524 (1982).
14. J. L. Merz and R. A. Logan, *J. Appl. Phys.*, **47**, 3503 (1976).
15. S. Adachi, H. Kawaguchi, and G. Iwane, *J. Mater. Sci.*, **16**, 2449 (1981).
16. J. L. Richard and A. J. Crocker, *J. Appl. Phys.*, **31**, 611 (1960).
17. B. Tuck, J. S. M. Mills, and A. J. Hartwill, *J. Mater. Sci.*, **11**, 847 (1976).
18. D. J. Stirland, *ibid.*, **9**, 969 (1974).
19. F. K-Kuhnenfeld, Inst. Phys. Conf. Ser. No. 33a, 158 (1977).
20. V. L. Rideout, *This Journal*, **119**, 1778 (1972).
21. D. W. Shaw, *ibid.*, **113**, 958 (1966).
22. I. Shiota, K. Motoya, T. Ohmi, N. Miyamoto, and J. Nishizawa, *ibid.*, **124**, 155 (1977).
23. T. Kobayashi and K. Sugiyama, *Jpn. J. Appl. Phys.*, **12**, 619 (1973).
24. M. M. Fakter, D. G. Fiddyment, and M. R. Taylor, *This Journal*, **122**, 1566 (1975).
25. C. J. Nuese and J. J. Gannon, *ibid.*, **117**, 1094 (1970).
26. J. C. Dyment and G. A. Rozgonyi, *ibid.*, **118**, 1346 (1971).
27. L. F. Eastman, R. Stall, D. Woodard, N. Dandekar, C. E. C. Wood, M. R. Shur, and K. Board, *Electron. Lett.*, **13**, 525 (1980).
28. S. Adachi, M. Kawashima, K. Kumabe, K. Yokoyama, and M. Tomizawa, *IEEE Electron Dev. Lett.*, **edl-3,** 409 (1982).

On the Structural and Luminescent Properties of the M′ $LnTaO_4$ Rare Earth Tantalates

L. H. Brixner and H.-y. Chen

E. I. du Pont de Nemours and Company, Central Research and Development Department, Experimental Station, Wilmington, Delaware 19898

ABSTRACT

The structure of M′ $YTaO_4$ has been redetermined and was refined to an R value of 0.034. M′ $YTaO_4$ crystallizes in P2/a symmetry with a = 5.298(1), b = 5.451(1), c = 5.111(1) Å, β = 96.45 deg. At temperatures >1450°C, M′ $YTaO_4$ will convert by way of a reconstructive transformation into the $I4_1/a$ symmetry of scheelite, and, upon cooling, a second-order ferroelastic transition (4/mF2/m) to M (fergusonite) $YTaO_4$ occurs. There are significant structural differences between M and M′ $YTaO_4$ which are discussed. M′ $LnTaO_4$ compounds exist from Ln = Sm to Lu. As a host for luminescent ions, M′ $YTaO_4$ is superior to the M modification, as well as all other compounds in the Y_2O_3/Ta_2O_5 phase diagram.

Structure

Contrary to the $LnNbO_4$-type rare earth niobates (1), which exhibit only one structural type (fergusonite) at room temperature, the tantalates crystallize in three different structures: the $P2_1/n$ type for La, Ce, and Pr (2); the fergusonite or M type (1) for Nd, Sm, Eu, Gd, Tb, Dy, Ho, and Er; and the M′ type (3) of Tm, Yb, and Lu. The latter type (M′) is the true equilibrium phase at room temperature, and all of the M-type tantalates (except Nd) also crystallize in this structure if prepared under appropriate conditions. In addition to these three structures, all $LnTaO_4$ tantalates convert to the $I4_1/a$ structure type (scheelite) at temperatures generally >1400°C.

Historically, Ferguson (4) in 1957 was first to describe both natural fergusonite (an yttrium-niobium-tantalate) as well as synthetic $YTaO_4$ correctly as crystallizing in monoclinic symmetry with the probable space group I2/a. This corrected the previous assumption originating with the morphological description by Haidinger (5) that fergusonite would be tetragonal and of scheelite type, which was also held by Barth (6) and Komkov (7). The first comprehensive listing of parameters for most $LnTaO_4$-type rare earth tantalates was given by Keller (1) in 1962. Keller could not characterize La, Ce, and $PrTaO_4$, as well as Tm, Yb, and $LuTaO_4$. The structure of the first three tantalates was reported by Wolten and Chase (2) to be $P2_1/n$, and the latter three tantalates could be structurally identified when Wolten (3) described yet another modification of $YTaO_4$ in the space group P2/a. Although Wolten (3) stated that this modification also exists for the tantalates of Sm to Yb, he did not report lattice parameters. Some of these (Er, Tm, Yb) appeared in the literature in form of ASTM file cards by McIlvried and McCarthy (8), who also described M′ $LuTaO_4$. The high temperature tetragonal ($I4_1/a$) modification of Nd, Sm, Gd, Tb, and $HoTaO_4$ was described by Stubican (9). In addition to the M′ structure of $YTaO_4$, we report here the cell dimensions of all $LnTaO_4$ compounds, both for the M and M′ forms, wherever they exist.

Key words: inorganic, crystallography, x-rays, luminescence.

Luminescence

While the luminescence of $CaWO_4$ was studied as early as 1897 (10), fluorescence properties of the rare earth tantalates were not mentioned in the literature until 1964 (11). Later on, extensive luminescence studies with the M (fergusonite) type rare earth tantalates (where Ln = Gd, Y, and Lu) were carried out by Blasse and Bril (12). These authors were primarily concerned with the energy and charge transfer processes of excitation via u.v. as well as electrons, and they recognized the NbO_4 group to be an efficient luminescent center in the fergusonite $YTaO_4$ host, where tetrahedral local site symmetry was assumed.

The dual purpose of the present paper was to confirm or correct Wolten's (3) structure for M′ $YTaO_4$, which was only refined to R = 15%, and to study the efficiency of some luminescing rare earths as well as